



At high  $\omega$  only the exchange term, namely (1c), is taken into account in the right hand side, while the so-called direct and time-reverse terms can be neglected contributing by the factor  $(I_{nl}/\omega)^2 \ll 1$  less [3]. The Eq. (2) has been solved numerically, using modified version of codes described in [5]. Note that the summation and integration over intermediate states  $\nu_3$  we performed numerically including nonrelativistic high energies  $\varepsilon_{\nu_3}$  that even exceed  $\omega$ .

Accurate solution of RPAE equations for unfilled shell atoms like Ni requires consideration of interaction of a large number of terms appearing after photoionization process. In this Letter the exact solutions of RPAE equations was replaced by configuration average approximation. This approximation makes possible to estimate general trends of electron correlation effects independent of a particular choice of the ground term. In this approximation the weight factors for the interaction between two open shells are obtained by multiplying the weight factors for filled shells by normalization factors  $(N_1 N_2)/[(4l_1 + 2)(4l_2 + 2)]$ , where  $N_{1,2}(l_{1,2})$  are numbers of electrons (angular momenta) of 1 and 2 interacting subshells. For the Coulomb interactions in one shell, the normalization factor  $N_1(N_1 - 1)/[(4l_1 + 2)(4l_1 + 1)]$  was used. Similar approach was employed for normalization of weight factors in angular parts of Coulomb interaction in (1).

The experimentally measured in [1] is the differential in angle photoionization cross section  $d\sigma_{nl}(\omega)/d\Omega$  that is determined by the following expression

$$\frac{d\sigma_{nl}(\omega)}{d\Omega} = \frac{\sigma_{nl}(\omega)}{4\pi} [1 + \beta_{nl}(\omega)P_2(\cos\theta) + \kappa\gamma_{nl}(\omega)P_1(\cos\theta) + \kappa\eta_{nl}(\omega)P_3(\cos\theta)]. \quad (3)$$

Here  $\sigma_{nl}(\omega)$  is the  $nl$ -subshell absolute photoionization cross-section,  $\kappa = \omega/c$ ,  $c$  is the speed of light,  $P_i(\cos\theta)$  are the Legendre polynomials,  $\beta_{nl}$  is the dipole while  $\gamma_{nl}$  and  $\eta_{nl}$  are the non-dipole angular anisotropy parameters,  $\theta$  is the angle between polarization vector and direction of photoelectron emission. In [1] the photon beam falls at  $2^\circ$  to the investigated sample surface and the photoelectron is detected along the polarization synchrotron radiation polarization vector. The plane created by the photon beam and polarization vector is orthogonal to the investigated sample surface.

Calculations of the cross-section and angular anisotropy parameters were performed for subshells  $nl = 3s$ ;  $3p$  and emission angle  $\theta = 0$ , using formulas from [4] modified by multiplying with presented above normalization factors. It appeared, in accord with the results of [6, 7] that the contribution of two last terms in

(3) is negligible. Therefore, instead of (3), considerably simpler expression was in fact measured

$$\frac{d\sigma_{nl}(\omega)}{d\Omega} = \frac{\sigma_{nl}(\omega)}{4\pi} [1 + \beta_{nl}(\omega)]. \quad (4)$$

**3. Specific of the experiments geometry.** In experiment the measurement was performed at such an angle that the really obtained quantity was, according to (4), not the photoionization cross-section  $\sigma_{3s,3p}(\omega)$ , but  $\sigma_{3s,3p}(1 + \beta_{3s,3p})$ . To derive the photoionization cross-sections in [1] the parameters  $\beta_{3s,3p}$  were taken from [3] and [4]. It appeared that they vary with  $\omega$  inessential, around 1 for  $\beta_{3p}$  and close to 2 for  $\beta_{3s}$ .

We have calculated the cross sections and angular anisotropy parameters, dipole and non-dipole, in the frame of one electron HF approach and with account of RPAE multi-electron correlations. The dipole parameters as well as cross-sections proved to be almost the same in HF and RPAE, thus signaling that the role of RPAE corrections is small enough. For  $3s$ -subshell  $\beta_{3s} = 2$ , while for  $\beta_{3p}(\omega)$  the following relation [4] was employed

$$\beta_{3p}(\omega) = \frac{D_{3p \rightarrow \varepsilon d}}{D_{3p \rightarrow \varepsilon s}^2 + 2D_{3p \rightarrow \varepsilon d}^2} \times [D_{3p \rightarrow \varepsilon d} - 2D_{3p \rightarrow \varepsilon s} \cos(\delta_s - \delta_d)], \quad (5)$$

where  $D_{3p \rightarrow \varepsilon d(s)}$  are the module of the dipole photoionization amplitude of the  $3p \rightarrow \varepsilon d(s)$  transitions, respectively and  $\delta_{d(s)}$  are the sums of amplitudes' and photoelectrons'  $d$  and  $s$  scattering phases.

**4. The results obtained.** Using (4) by substituting there dipole angular anisotropy parameters, the  $3s$  and  $3p$  photoionization cross-sections were obtained. In [1] the  $\beta$  parameters were taken from [6, 7]. Fig. 1 shows the result obtained for  $\sigma_{3s}(\omega)$  and  $\sigma_{3p}(\omega)$ , measured and calculated. On the same Fig. 1 we present results of [2] and in HF – Slater approximation [6, 7]. We see in experiment essential difference, noticeable even in logarithmic scale, between photoionization of Ni thin films and crystal samples. As to calculations, they were performed for an isolated Ni atom.

Calculations demonstrate that in the considered photon energy range, 2–10 keV, the role of RPAE correlations is almost negligible. In the same logarithmic scale there is no difference between HF-Slater and RPAE results. The data from [2] is closer to experiment than RPAE results.

Comparison between theory and experiment demonstrates reasonable agreement for  $3p$ -subshell. For  $3s$ -subshell, the relative difference between theory and experiment is steadily and very slow increasing with the

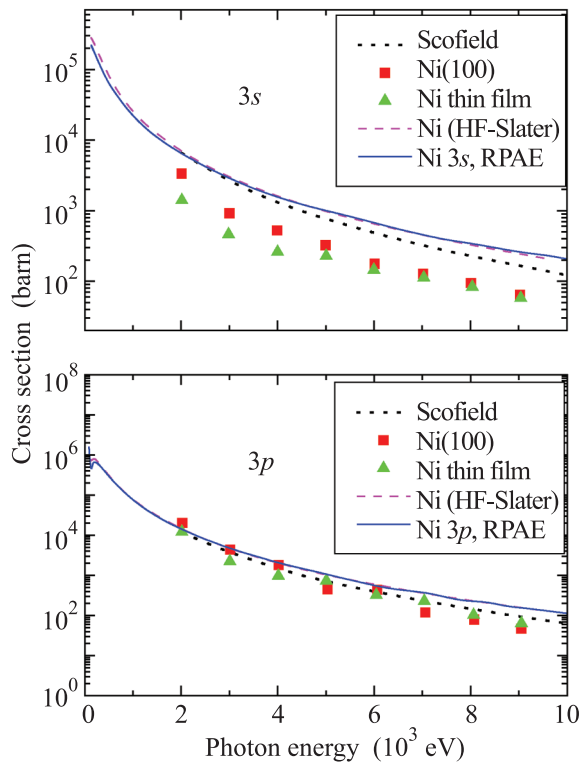


Fig. 1. The photoionization cross sections of  $3s$  and  $3p$  Ni subshells, measured in thin films and solid body, along with different calculation data

photon energy growth. This difference is big, the experimental value being smaller than the calculated one by a factor of 2.5–3.

As is seen from Fig. 1, for  $3p$ -subshell the deviation between results of calculation and measurement is much smaller than in the  $3s$ -case. In the entire considered photon energy interval, the measured cross section is smaller than the calculated and the difference slowly increases with  $\omega$  growth.

Fig. 2 shows the result directly observed in experiment: values of the ratio  $\sigma_{3s}(1 + \beta_{3s})/\sigma_{3p}(1 + \beta_{3p})$ , both measured [1] and calculated. On the same Figure along with our calculations we present results derived from [2] and in HF – Slater approximation [6, 7]. As is mentioned above, we put  $\beta_{3s} = 2$ . The linear instead of logarithmic scale permits to see the differences between theory and experiment more clearly. In the entire considered photon energy region the ratio increases. Since the role of angular anisotropy parameters in the presented in Fig. 2 ratio is important but, as it is seen in Fig. 3, depends upon photon energy weakly, the linear increase of  $\sigma_{3s}(1 + \beta_{3s})/\sigma_{3p}(1 + \beta_{3p})$  in the region  $\omega = 1–10$  KeV reflects the linear increase of the ratio  $\sigma_{3s}/\sigma_{3p}$  in the hydrogenlike approximation. It is seen that our results as well as that from [6, 7] are consider-

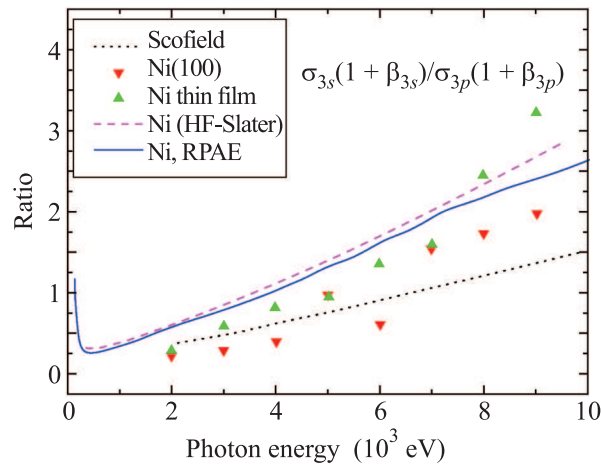


Fig. 2. The results of measurements [1] and calculation data for the ratio  $\sigma_{3s}(1 + \beta_{3s})/\sigma_{3p}(1 + \beta_{3p})$  in Ni film and crystal

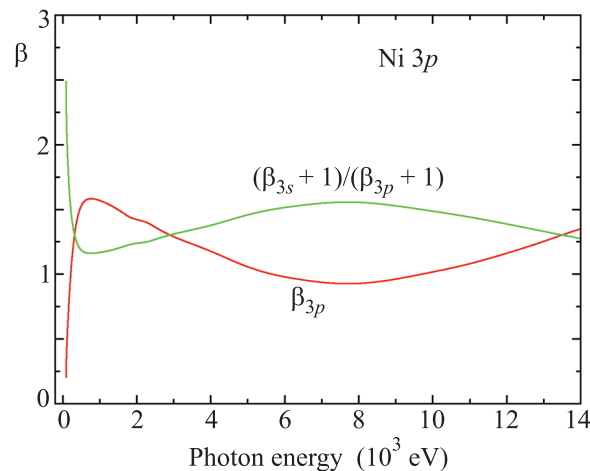


Fig. 3. Angular anisotropy parameter of Ni  $3p$ -electrons and the ratio  $(1 + \beta_{3s})/(1 + \beta_{3p})$

ably higher than that of [2]. The small role of electron correlations is clearly seen.

As to experimental data, they are considerably deviating from the linear law. Starting from 5 KeV the data for Ni film increases much faster than a simple,  $\sim \omega$ , function. The same is valid for the crystal Ni data, if imagine a smooth curve that goes with the smallest possible deviation via the experimental Ni bulk points.

It is seen that the RPAE results are in general closer to the thin film data. The results for crystal Ni up to 6 KeV are closer to the data of [2] than to RPAE and only at higher  $\omega$  lie closer to RPAE. Entirely, the linear scale emphasizes deviation between calculation and experimental data even more clear than the logarithmic scale of Fig. 1.

As is seen from Fig. 3, the increase of  $\beta_{3p}$  is fast below  $\approx 800$  eV, but in the whole considered photon energy region  $\omega = (2-15)$  keV it varies slowly from 1.5 to about 1 and back, having a broad shallow minimum. As to the cross sections they decrease in the same photon energy region monotonically by several orders of magnitude.

**5. Concluding remarks.** As is evident from Figs. 1 and 2, neither HF nor RPAE are able to describe the experimental data for the absolute values of the cross-sections or their ratio. Since the dynamic correlations rapidly die out with photon energy increase, is hard to believe that these correlations can be responsible for the observed difference.

On the way out, the photoelectron can collide with the residual ion inelastic, or even lead to collective excitation of the target. However, such effects were studied in connection to Xe photoionization [9]. For high energy photoelectrons they would contribute similarly for  $3s$ - and  $3p$ -photoionization and the corresponding effect would decrease as  $1/E$ . Obviously this is not what was observed in [1].

As it was demonstrated in [3], there exist some RPAE corrections that could be of importance at high  $\omega$ . However these are not affecting  $3s$  cross-section and in principle could increase the  $3p$  cross-section, which is already too big.

Of importance could be the effect of the so-called spectroscopic factor  $F_{nl} < 1$  of a  $nl$ -level, even of an  $s$ -level [10]. This factor represents an admixture due to electron correlations of other levels or of the continuous spectrum to the considered  $nl$ -level. It modifies the cross-section simply by multiplying its RPAE value by  $F_{nl}$ . Thus, in order to achieve agreement with experimental data one needs  $F_{3s} \approx 0.3$  that is unlikely. At least direct calculation for Ni neighbor, Mn atom, gives for  $F_{3s}$  a considerably bigger value close to 0.7 [10]. Calculations of interaction between final state configurations  $3s^{-1}$  and  $3p^{-2}3d^{+1}$  [11] resulted in that only 0.05 of the Ni  $3s$ -spectrum is pushed to high binding energy and not included in the analyzed spectral region. Thus, the theoretical results [10,11] rule out that the big difference between theory and experiment could be explained by inclusion of the spectroscopic factor. Note, that the measured in [1] structure of  $3s$ -level also excludes the smallness of  $F_{3s}$  and its important role.

At first glance, a little bit suspicious is the limitation in the angular distribution (4) by dipole and quadrupole corrections only. Indeed, the corresponding multipole expansion parameter can be estimated as 0.2. It is not too small but makes the large contribution of the term of second power in  $\kappa$ , neglected in (4), unlikely. This conclusion is confirmed by calculations in [7] that included the  $\kappa^2$  terms, which proved to be three orders of magnitude smaller.

The strong influence of the shape of the sample, namely, whether it is a crystal or a film surprises also. For levels with binding energy of 110 eV (for  $3s$ ) and 67 eV (for  $3p$ ) a strong effect of location of neighboring atoms looks almost improbable.

Entirely, the investigation of atomic photoionization in the tens keV region requires and deserves further efforts and clarifications, both theoretical and experimental.

1. A. M. Gorgoi, F. Schafers, S. Svensson, and N. Martensson, *J. Electron Spectroscopy & Related Phenomena* (2013); <http://dx.doi.org/10.1016/j.elspec.2013.01.004>.
2. J. H. Scofield, *Lawrence Livermore National Laboratory Report*, UCRL-51326, 1973.
3. M. Ya. Amusia, N. B. Avdonina, E. G. Drukarev et al., *Phys. Rev. Lett.* **85**, 4703 (2000).
4. M. Amusia, L. Chernysheva, and V. Yarzhemsky, *Handbook of Theoretical Atomic Physics*, Springer-Verlag, Berlin, Heidelberg, 2013.
5. M. Ya. Amusia and L. V. Chernysheva, *Computations of Atomic Processes*, Bristol and Philadelphia, IOP publishing, 1997.
6. M. B. Trzhaskovskaya, V. I. Nefedov, and V. G. Yarzhemsky, *At. Data and Nuclear Data Tables* **77**, 97 (2001).
7. M. B. Trzhaskovskaya, V. I. Nefedov, and V. G. Yarzhemsky, *At. Data Nuclear Data Tables* **82**, 257 (2002).
8. M. Ya. Amusia, *Atomic Photoeffect*, N.Y.-London, Plenum Press, 1990.
9. M. Ya. Amusia, G. F. Gribakin, K. L. Tsemekhman, and V. L. Tsemekhman, *J. of Phys. B: At. Mol. Opt. Phys.* **23**(3), 393 (1990).
10. M. Ya. Amusia and V. K. Dolmatov, *J. Phys. B: At. Mol. Opt. Phys.* **26**, 1425 (1993).
11. E. K. Viinikka and Y. Ohn, *Phys. Rev. B* **1**(11), 4168 (1975).